Electronic Letters on Computer Vision and Image Analysis 10(1):1-10, 2011

Implementation of Max Principle with PCA in Image Fusion for Surveillance and Navigation Application

Senthil Kumar Sadhasivam*, Mahesh Bharath Keerthivasan# and Muttan S+

** Dept of Electronics and Communication Engineering, St. Joseph's College of Engineering, Chennai, India*
 # Dept of Electrical and Computer Engineering, The University of Arizona, Tucson,United States
+ Dept of Electronics and Communication Engineering, College of Engineering, Anna University, Chennai, India

Received 11th November 2010; accepted 17th June 2011

Abstract

Image fusion is the combination of two or more different images by using suitable algorithms to form an output image. It provides a useful tool to integrate multiple images into a composite image. In this paper, we present an approach that uses the principle component analysis (PCA) along with the selection of maximum pixel intensity to perform fusion. The entropy, mutual information and the universal index based measure are used to evaluate the performance of this fusion algorithm.

Key Words: pixel level image fusion, Principal Component Analysis, weight based fusion

1 Introduction

Image fusion process can be defined as the integration of information from a number of registered images without the introduction of distortion [1]. One of the goals of image fusion is to create a single enhanced image more suitable for the purpose of human visual perception, object detection and target recognition. This fusion of images obtained from different modalities is of great importance in applications such as medical imaging, remote sensing and machine vision [2, 3].

Image fusion systems are widely used in surveillance and navigation applications, for both military and domestic purposes. This is achieved by the use of multiple sensors to obtain the visual information and by utilizing the synergism of different imaging sensors for better situation assessment [4]. Presently, the focus is on the fusion of infrared (IR) images along with visible images obtained using charge coupled device (CCD) cameras [1, 5]. The infrared image is a map of the infrared radiations which are emitted by objects having a temperature above absolute zero, the amount of radiation emitted being partly governed by the object's temperature. Hence, warm objects like humans can be detected easily in an infrared image. However, to image objects such as trees, leaves or grass in a natural scene low light visible cameras are the preferred choice. Thus there is a need for visual information integration and multi-sensor image fusion gives a promising solution.

In the image fusion process multi-sensor outputs can be combined to give a better quality image of the scene. Image fusion is generally divided into three categories; pixel level, feature level and decision level

Correspondence to: <ssk_puliyur@yahoo.com>

Recommended for acceptance by <Xavier Otazu>
ELCVIA ISSN: 1577-5097
Published by Computer Vision Center / Universitat Autonoma de Barcelona, Barcelona, Spain

fusion [6, 7]. Pixel level fusion works directly on the pixels obtained at imaging sensor outputs while feature level fusion algorithms operate on features extracted from the source images. Decision level fusion uses the outputs of initial object detection and classification as inputs to the fusion algorithm to perform the data integration. Both feature level and decision level image fusion may result in inaccurate and incomplete transfer of information [6, 7]. In this paper, we focus on pixel level fusion.

A considerable number of approaches to multi-sensor image fusion have been discussed in the literature. These are broadly classified under multi-resolution analysis (MRA) based fusion, statistical techniques based fusion and fuzzy logic based fusion. The MRA fusion approach includes the Laplacian pyramid algorithm [8], the gradient pyramid algorithm [9] and the discrete wavelet transform algorithm [10, 11]. Under the statistical fusion schemes are the principle component transform (PCA) analysis, regression variable substitution [12, 13] and the canonical variate substitution [14] algorithms. Burke developed an image fusion algorithm using principle component analysis [15] and Das et al. proposed a PCA based image fusion technique for night vision application [16]. Also hybrid techniques have been proposed; such as the advanced wavelet transform (aDWT) method by Zheng et al. [17] that incorporates principle component analysis and morphological processing into a regular DWT fusion algorithm. The use of PCA based fusion with wavelet decomposed images has been discussed by Gonzalez-Audicana et al. [18]. A more comprehensive description of the recent fusion methods is available in [19, 20, 21, 22]. The authors have already proposed the use of a weighted based PCA fusion scheme [23].

The subsequent sections of this paper are organized as follows. In section 2, the author's weighted PCA fusion method is discussed. In Section 3, a new fusion technique based on PCA is proposed. Section 4 describes the metrics used for evaluating the fused images and gives the experimental results obtained. The final section concludes the paper.

2 The weighted principle component analysis (PCA) fusion method

The principle component analysis is a mathematical way of determining the linear transformation of a sample of points in a *N*-dimensional space exhibiting the properties of the sample along the coordinate axes. It enables a decrease in the number of channels (or images) by reducing the inter-channel dependencies. This analysis is based on the computation of the covariance matrix and its diagonalization by finding corresponding eigenvalues and eigenvectors. The first eigenvector (or principle component) is a linear combination of the initial images and usually contains more than 90% of the information contained in all the images. Two sets of data can then fused by concatenating all channels and performing a PCA transformation on all the channels to keep only the non-redundant information.

A weighted fusion algorithm using PCA has been described by the authors in [23]. Here the IR and visible source images, Iir and Ivis, are initially smoothened using a gaussian filter to separate the high frequency and the low frequency components. The smoothened low frequency images are denoted by Sir and Svis. The high frequency edge components, denoted by Dir and Dvis, are obtained as the difference between source image and the smoothened image. The covariance matrix of the difference image data vectors is calculated. The principle eigenvector, corresponding to the maximum eigenvalue of the covariance matrix is determined. The components of the principle eigenvector are used as the weights wir and wvis.

The fused image is composed by averaging the smoothed input images and adding the weighted, normalized sum of the deviations.

$$M = \left(S_{ir} + S_{vis}\right) / \ 2 \ + \ \left[\left(D_{ir} * w_{ir}\right) \ + \ \left(D_{vis} * w_{vis}\right)\right] \ / \ \left(w_{ir} + w_{vis}\right) \qquad (1)$$

The weights w_{ir} and w_{vis} are defined by equations (11) and (12) as explained in Section 3. While this algorithm has been found to be efficient than the simple additive fusion [24] and Laplacian pyramid algorithm [8], it gives a reduced performance when compared with the hybrid DWT - PCA fusion algorithm proposed by Zheng et al. [25].

3 Proposed fusion technique: PCA - Max fusion

The new scheme overcomes the performance limitation of the DWT - PCA fusion algorithm [25] and the PCA weighted fusion method [23]. This is achieved by using the author's previously reported PCA based weighted fusion technique [23] along with the Select Max principle outlined in [25] to improve the fusion accuracy.

The source images, I_{ir} and I_{vis} of size M x N each, are passed through a Gaussian low pass filter to give the smoothened images

$$S_{vis} = I_{vis} * \exp\left[-\left(x^2 + y^2\right)/\sigma^2\right] \quad (2)$$

$$S_{ir} = I_{ir} * \exp\left[-\left(x^2 + y^2\right)/\sigma^2\right] \quad (3)$$

The high frequency difference image is obtained by calculating the deviation of the smoothened images from the source image.

$$D_{vis} = I_{vis} - S_{vis} \quad (4)$$

$$D_{ir} = I_{ir} - S_{ir} \quad (5)$$

The low frequency images S_{ir} and S_{vis} are fused using the 'Select Max' principle as discussed by Zheng et al. in [25]. Since the visible information is contained in the low frequency components, fusing the images by selecting the pixel values with the highest intensity gives an output image that has a very high quality as perceived by the human observer. However, to enable comparison of the images on a pixel by pixel basis a histogram matching of the two images is performed. This is achieved by matching the visible image's histogram to that of the IIR image.

The decision map of the low frequency image fusion rule of choosing the maximum intensity pixel values is represented mathematically as:

$$S_{fuse}(m,n) = \begin{cases} S_{ir}(m,n), \text{ if } S_{ir}(m,n) > S_{vis}(m,n) \\ S_{vis}(m,n), \text{ if } S_{ir}(m,n) < S_{vis}(m,n) \end{cases} \quad (6)$$

The high frequency difference images D_{ir} and D_{vis} are fused using the weighted average rule, the weights being determined by applying the PCA to the images. Firstly, the two images, D_{ir} and D_{vis} of dimension MxN each, are stacked and the pixels extracted from the corresponding locations are organized into an array X, of dimension MN x 2. The next step is the computation of mean vector of the population, which is defined by the equation

$$m_x = \left(\frac{1}{M}\right)\sum_{k=1}^{M} x_k \quad (7)$$

where, K = M x N

For M vector samples from a random population, the covariance matrix can be approximated from the samples by

$$C_x = \left(\frac{1}{M}\right)\sum_{k=1}^{M}\left[x_k x_k^T - m_x m_x^T\right] \quad (8)$$

Because C_x is real and symmetric, finding a set of n orthogonal eigenvectors always is possible. Let e_i and λ_i, i = 1,2…n, be the eigenvectors and corresponding eigenvalues of C_x, arranged in descending order so that $\lambda_j \geq \lambda_j + 1$ for j = 1,2…n-1.

Let A be a matrix whose rows are formed from the Eigen vectors of C_x ordered so that the first row of A is the Eigen vector corresponding to the largest eigenvalue and the last row is the eigenvector corresponding to the smallest eigenvalue.

Suppose that A is a transformation matrix that maps the x's into vectors denoted by y's,

$$Y = A(x - m_x) \tag{9}$$

This equation is called the principle component transform. The mean of the y vectors resulting from this transformation is zero and the covariance matrix of the y's can be obtained in terms of A and C_x by

$$C_y = A \cdot C_X \cdot A^T \tag{10}$$

Furthermore, C_y is the diagonal matrix whose elements along the main diagonal are eigenvalues of C_x; that is,

$$C_y = \begin{bmatrix} \lambda_1 & 0 & 0 \\ 0 & \lambda_2 & 0 \\ 0 & 0 & \lambda_3 \end{bmatrix} \tag{11}$$

The off-diagonal elements of the covariance matrix are 0, so the elements of the y vectors are uncorrelated. The rows of matrix A are the normalized eigenvectors of C_x. Because C_x is real and symmetric, these vectors form an orthonormal set, and it follows that the elements along the main diagonal of C_y are the eigenvalues of C_x. The main diagonal element in the i^{th} row of C_y is the variance of vector element y_i.

The Eigen values for each principle component correspond to the amount of total variance in the data described by this component [26]. Then the weights, w_{ir} and w_{vis}, are obtained by smoothening the eigenvalues $\lambda 1_{\text{ and }} \lambda_2$ as defined by the authors in [23],

$$w_{vis} = \lambda_1 * \exp\left[-\left(x^2 + y^2\right)/\sigma^2\right] \tag{12}$$

$$w_{ir} = \lambda_2 * \exp\left[-\left(x^2 + y^2\right)/\sigma^2\right] \tag{13}$$

The fused high frequency components is obtained using

$$D_{fuse} = \frac{(D_{ir} \cdot w_1) + (D_{vis} \cdot w_2)}{[w_1 + w_2]} \tag{14}$$

The final fused image is the obtained by adding the fused low frequency and fused high frequency images together

$$I_{fuse} = S_{fuse} + D_{fuse} \tag{15}$$

4 Performance Evaluation and Results

The objective quality metrics used to evaluate image fusion performance are broadly classified as full - reference assessment methods and non -reference assessment methods. The full-reference approaches

compare the fused image with a distortion free reference image of the same scene, as produced by a perfect fusion scheme. Some of the full-reference metrics reported in the literature are Wang's Image Quality Index [27], the Root Mean Square Error (RMSE), Peak Signal to Noise Ratio (PSNR), Image Fidelity (IF) [28] and the Mean Absolute Error (MEA).

The fusion algorithms outlined in this paper are directed towards applications in the areas of surveillance and navigation. In these applications, due to the real-time nature of the scene being imaged, there are no ground truth data available. Hence, evaluating the performance of such fusion schemes requires the use of non-reference quality metrics. Accordingly, we have used three parameters to measure the efficiency of our namely, the entropy of the image [29], the mutual information [30] and the Structural Similarity (SSIM) Index based measure (SI) [31].

4.1 Entropy

The entropy is used to measure the information content of an image [29] and has been used by Leung et al. [32] to measure the performance of image fusion. The entropy of an image is given by

$$E_n = \sum_{j=0}^{G} p(i) \log_2 p(i) \tag{16}$$

Where, G is the number of gray levels in the image and p(i) is the normalized probability of occurrence of each gray level.

4.2 Mutual Information

This metric is calculated by defining the joint histogram of the source image I_{ir} , I_{vis} and the fused image I_{fuse} as p(fuse,ir) and p(fuse,vis). The mutual information between the source image and the fused image is given by [30] as

$$Mi_1(fuse,ir) = -\sum p(fuse,ir) \log_2 \left(\frac{p(fuse,ir)}{p(fuse).p(ir)} \right) \tag{17}$$

$$Mi_2(fuse,vis) = -\sum p(fuse,vis) \log_2 \left(\frac{p(fuse,vis)}{p(fuse).p(vis)} \right) \tag{18}$$

where, p(fuse, ir) and p(fuse, vis) are the joint histograms of the source image I_{ir} , I_{vis} and the fused image I_{fuse}

The fusion algorithm efficiency is determined by the metric MI which is defined by

$$MI = Mi_1(fuse,ir) + Mi_2(fuse,vis) \tag{19}$$

4.3 SSIM index based measure (SI)

The SSIM index proposed by Wang and Bovik [33] is used as an objective image quality metric to indicate the similarity of the structure information present in the two images being compared. The SSIM of two images x and y is defined as

$$SSIM(x,y) = \frac{(2\mu_x\mu_y + C_1)(2\sigma_{xy} + C_2)}{(\mu_x^2 + \mu_y^2 + C_1)(\sigma_x^2 + \sigma_y^2 + C_2)} \tag{20}$$

where, μ is the mean intensity of the image, σ is the standard deviation of the image and C_1, C_2 are constants

However, the SSIM is a full-reference approach and requires the need for a complete reference image for its calculation. This impediment is overcome by separately calculating the amount of structure information transferred from each of the source images to the fused image, SSIM(fuse, ir) and SSIM(fuse, vis) [31]. Then the SSIM index for the fused image is calculated by

$$SI = SSIM(fuse, ir) + SSIM(fuse, vis) \quad (21)$$

5 Experimental Tests and Results

We tested the proposed algorithm on a set of three different images and measured the parameters that determine the performance of the fusion. The effectiveness of the proposed scheme is determined by comparing it with the author's weighted PCA method [23] and the DWT - PCA method as outlined in [25]. The images used for experimentation, the UN camp, road and boat images. The road and boat images pertain to scenes captured during the night time. As can be seen, the visible image captured using a normal camera shows the bright light source obscuring the objects in the scene. The IR image on the other hand gives a clear outline of the object present with the necessary details. The UN camp image is an example of a surveillance image, wherein the presence of a person hiding behind the bush is outlined in the IR source image.

These images were obtained from the multi-sensor image segmentation data set [34] and have been registered before fusion to avoid any error due to mis-registration of the images. Registration was performed in a semi-automatic manner using the IMARE registration toolbox with the invariant based method [35]. Parameters used to compute the invariants were chosen by the authors for every image pair and the RMSE was used to evaluate the registration accuracy.

Figures 1a, 1b shows the IR and visual source image of a boat taken during the night time. The result of fusing the two images using the various methods is shown in Figures 1 c-e. The metrics are calculated for the different fusion algorithms and are shown in Table 1. The values show that the proposed method has a very good performance and this is validated by the subjective quality of the fused image.

(a)	(b)	(c)
(d)		

Figure 1: Fusion Results: (a) Original IR image (b) Original CCD image (c) PCA Fusion (d) DWT-PCA Fusion (e) Proposed PCA-Max Fusion

The images in Figure 2 show a road during the night time. The roofs of the houses are visible in the IR image which also shows a man standing on the road. The CCD image is unclear because of the effects of the bright street lights. The resultant fused images obtained by using the various algorithms are shown in Figures 2c – 2e.

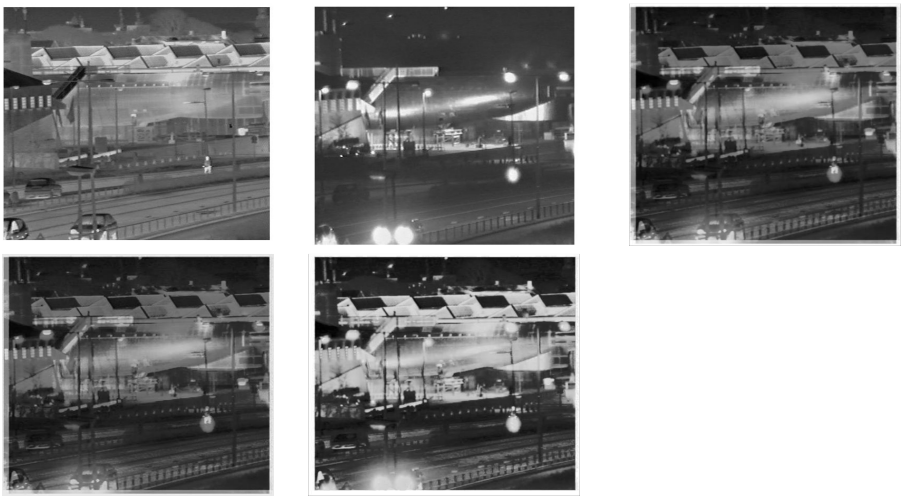

(a)	(b)	(c)
(d)		

Figure 2: Fusion Results: (a) Original IR image (b) Original CCD image (c) PCA Fusion (d) DWT-PCA Fusion (e) Proposed PCA-Max Fusion

The third data set in Figure 3 is the picture taken of a UN camp. The IR image shows a man hiding amongst the bushes. The CCD visible image shows the fence around the house. The fused image obtained using the various algorithms are shown in Figures 3c –3e.

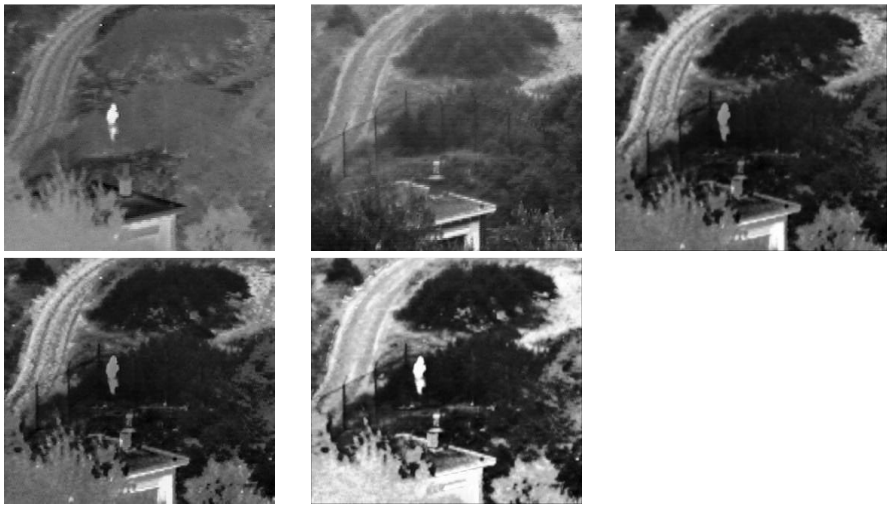

(a)	(b)	(c)
(d)		

Figure 3: Fusion Results: (a) Original IR image (b) Original CCD image (c) PCA Fusion (d) DWT-PCA Fusion (e) Proposed PCA-Max Fusion

Image	Fusion Technique	Entropy	SSIM based measure	Mutual Information
Boat (Figure 1)	**PCA Max Fusion**	**7.58349**	**0.664093**	**4.46357**
	PCA weighted fusion	7.32242	0.684189	3.05004
	PCA DWT Fusion	7.29356	0.282595	3.10495
Road (Figure 2)	**PCA Max Fusion**	**7.42964**	**0.649915**	**4.03913**
	PCA weighted fusion	7.37228	0.664613	2.79379
	PCA DWT Fusion	7.26513	0.25205	2.76195
UN camp (Figure 3)	**PCA Max Fusion**	**7.63398**	**0.591599**	**3.65789**
	PCA weighted fusion	7.18519	0.58918	2.47197
	PCA DWT Fusion	7.14714	0.250342	2.50575

Table 1: Comparison of the performance of fusion algorithms

The results in Table 1 validate the efficiency of the proposed fusion scheme. While the entropy of the fused output is similar for all the three techniques the proposed PCA Max fusion method has a performance better than the existing DWT – PCA method [25] in terms of the structural similarity and amount of information transferred onto the fused image. Compared to the author's PCA weighted algorithm [23] the proposed method shows an improvement in the mutual information of the fusion output while the SSIM measure remains approximately at the same level. This can be attributed to the fact that the selection of maximum intensity pixels transfers more information than a simple PCA weighting.

6 Conclusion

In this paper, we put forward a new pixel level image fusion algorithm using the PCA technique. We have compared the performance of our method with some of the recent PCA based fusion schemes. The effectiveness of the fusion rule is determined by the objective evaluation of the fusion performance using parameters such as the entropy, mutual information and the SSIM based index. From the experiments conducted and human observation of the fused images we conclude that the proposed PCA - Max fusion algorithm is an efficient technique for fusing IR and visible spectrum images.

References

[1] A. Haq, A.M. Mirza and S. Qamar, An Optimized Image Fusion Algorithm For Night-Time Surveillance And Navigation, Proceedings of the International Conference on Emerging Technologies, Islamabad, 2005, pp138-143

[2] G. Pajares, J.M. de La Cruz, A Wavelet Based Image Fusion Tutorial, Pattern Recognition, 37, 2004, pp.1855-1872

[3] C. Pohl, and J.L. VanGenderen, Multisensor Image Fusion in Remote Sensing : Concepts, Methods and Applications, International Journal of Remote Sensing Vol. 19, No. 5, 2008, pp. 823-854

[4] G.H. Harris and L.C. Graham, Landsat-Radar Synergism, Proceedings of the XII Congress of ISP, 1976, Helsinki, Finland

[5] S. Das, Y-L. Zhang, W.K. Krebs, Color night vision for navigation and surveillance, Proceedings of the fifth joint conference on information science, Atlantic City, NJ, Feb 2000

[6] G. Piella, A General Framework For Multi-Resolution Image Fusion: From Pixels To Regions, Information Fusion, 9, Dec 2003, pp. 259-280

[7] Lawrence A. Klein, Sensor and Data Fusion: A Tool for Information Assessment and Decision Making, SPIE, vol.PM138-H.Li.B.

[8] P.J. Burt and E.H. Adelson, The Laplacian Pyramid as a Compact Image Code, IEEE Transaction on Communications, 31(4) : 532-540, 1983

[9] P.J. Burt, A Gradient Pyramid Basis for Pattern Selective Image Fusion, Society for Information Display, Digest of Technical Papers, pp. 467-447,1992

[10] T. Huntsberger and B. Jawerth, Wavelet Based Sensor Fusion, Proceedings of SPIE, vol.2059, pp. 488-498, 1993

[11] K. Amolins, Y. Zhang and P. Dare, Wavelet based image fusion techniques – An introduction, review and comparison, ISPRS Journal of Photogrammetry and Remote Sensing, vol.62, issue 4, pp. 249-263

[12] V.K. Shettigara, A Generalized Component Substitution Technique for Spatial Enhancement of Multispectral Images using a Higher Resolution Data Set, potogrammetric Engineering and Remote Sensing,vol.58, pp. 561-567, 1992

[13] A. Singh, Digital Change Detection Techniques Using Remotely Sensed Data, International Journal of Remote Sensing, vol.10, pp. 989-1003, 1989

[14] N.A. Campbell, Towards More Quantitative Extraction of Information from Remotely Sensed Data, Proceedings of Conference in Advanced Remote Sensing, Sydney, vol. 2, pp.29-40, 1993

[15] S.M. Hsu and H. K. Burke, Multisensor Fusion with Hyperspectral Imaging Data: Detection and Classification, Lincoln Laboratory Journal, Vol. 14, No. 1, 2003, pp. 145 – 159

[16] S. Das, Y-L. Zhang, W.K. Krebs, Color night vision for navigation and surveillance, Proceedings of the fifth joint conference on information science, Atlantic City, NJ, Feb 2000

[17] Y. Zheng, E. A. Essock and B.C. Hansen, An advanced Image Fusion Algorithm Based On Wavelet Transform - Incorporation with PCA and Morphological Processing, Proceedings of the SPIE, Vol. 5298 (2004) pp.177-187.

[18] M. Gonzalez-Audicana, J.L. Saleta, R.G. Catalan and R. Garcia, Fusion of multispectral and panchromatic images using improved HIS and PCA mergers based on wavelet decomposition, IEEE Transactions on Geoscience and Remote Sensing, 42 (6), pp. 1291-1299

[19] M.I. Smith and J.P. Heather, A review of image fusion technology in 2005, Proc. SPIE 5782, 29 (2005)

[20] D.L. Hall. and J. Llinas, Multisensor Data Fusion, In Handbook of Multisensor Data Fusion Theory and Practice, 2 ed., 2008, CRC Press, pp. 1-14.

[21] H.B. Mitchell, Image Fusion: Theories, Techniques And Applications, Springer, 2010

[22] J. Zeng, A. Sayedelahl, T. Gilmore and M. Chouikha, Review of Image Fusion Algorithms for Unconstrained Outdoor Scenes, Signal Processing, 8th International Conference on , vol.2, no., 16-20 2006

[23] S. Senthil Kumar and S. Muttan, PCA Based Image Fusion, Proceedings of SPIE, vol. 6233, pp. 62331T-1 to 62331T-8

[24] E.J. Bender, C.E. Reese and G.S. van der Wal, Comparison of Additive Image Fusion Versus Feature Level Image Fusion Techniques for Enhanced Night Driving, Proceedings of SPIE Conference on Low-Light-Level and Real-Time Imaging Systems, Components, and Applications, Seattle, USA, July 2002, Vol. 4796, pp. 140-151

[25] Y. Zheng, X. Hou, T. Bian and Z. Oin, Effective Image Fusion Rules of Multiscale Image Decomposition, Proceedings of the 5th International Symposium on Image and Signal Processing and Analysis, pp. 362 – 366, 2007

[26] R.C. Gonzalez, R.E. Woods and S.L. Eddins, Digital Image Processing Using MATLAB, Pearson Education Inc., 2004

[27] Z. Wang and A.C. Bovik, A universal image quality index, IEEE Signal Processing Letters, Vol. 9, No. 3, pp. 81-84.

[28] K. Kannan and S. Arumuga Perumal, 'Optimal Decomposition Level of Discrete Wavelet Transform for Fusion of Multi-focussed Images', Proceedings of the International Conference on Computational Intelligence and Multimedia Applications, December 2007, Sivakasi, India, Vol. 3, pp. 314-318.

[29] A. Renyi, On Measures of Entropy and Information, Proceedings of the 4th Berkeliey Symposium on Mathematics Statistics and Probability, vol.1 , pp. 547- 561, 1961

[30] G. Qu, D. Zhang and P.Yan, Information Measure for Performance of Image Fusion,Electronic Letters, 38(7), pp. 313-315, 2002

[31] R. Maruthi and R.M. Suresh, 'Metrics for Measuring the Quality of Fused Images', Proceedings of the International Conference on Computational Intelligence and Multimedia Applications, December 2007, Sivakasi, India, Vol. 3, pp. 153-158.

[32] L.W. Leung, B. King and V. Vohora, Comparison of Image Data Fusion Techniques Using Entropy and INI, 22nd Asian Conference on Remote Sensing, 2001, 5-9 November

[33] Z. Wang, A.C. Bovik, H.R. Sheik and E.P. Simoncelli, Image Quality Assessment: From error visibility to structural similarity, IEEE Transactions on Image Processing, Vol. 13, No. 4, 2004, pp. 600-612

[34] J. J. Lewis, S. G. Nikolov, A. Toet, D. R. Bull and C. N. Canagarajah, Uni-modal versus joint segmentation for region-based image fusion, Proceedings of the 9th International Conference on Information Fusion, (Fusion 2006), Florence (Italy), 10-13 July 2006

[35] B. Zitová and J. Flusser, IMARE - image registration toolbox for MATLAB, Freeware, http://www.utia.cas.cz/user_data/zitova/IMARE.htm